

## Simultaneous Noninvasive Measurement of Blood Flow in the Great Cardiac Vein and Left Anterior Descending Artery

---

Willemijn L. F. Bedaux,<sup>1,3</sup> Mark B. M. Hofman,<sup>2</sup>  
Cees A. Visser,<sup>1,4</sup> and Albert C. van Rossum<sup>1,3,4</sup>

<sup>1</sup>Department of Cardiology and <sup>2</sup>Department of Clinical Physics & Informatics, University Hospital Vrije Universiteit, Amsterdam, The Netherlands

<sup>3</sup>Interuniversity Cardiology Institute Netherlands, Utrecht, The Netherlands

<sup>4</sup>Institute for Cardiovascular Research ICaR-VU, Amsterdam, The Netherlands

### ABSTRACT

Magnetic resonance (MR) flow mapping can be used to quantify flow velocity and volume flow in the coronary vessels noninvasively. The close anatomic relationship of the left anterior descending artery (LAD) with the great cardiac vein (GCV) allows imaging of both in one view. We examined the feasibility to discriminate between these two vessels based on the flow pattern and to measure the flow quantitatively. Eleven individuals with a normal LAD and 8 patients with a diseased LAD underwent MR imaging. From MR angiograms using connectivity to the aortic root, differentiation between the LAD and GCV was obtained. Perpendicular to both vessels, phase-contrast velocity mapping was performed to measure phasic and mean volume flow. After correction for cardiac motion of the vessel, GCV flow was found to be mainly systolic and pointing in the inverse direction as the predominantly diastolic flow in the LAD. These criteria appeared valid in all subjects, even in cases of highly stenotic arteries. The volume flow measurements corrected for body surface area were  $31 \pm 15$  ml/min/m<sup>2</sup> in the normal LAD (n = 11) and  $21 \pm 10$  ml/min/m<sup>2</sup> in the diseased LAD (n = 7). The volume flow measurements in the GCV

Address correspondence and reprint requests to Willemijn L. F. Bedaux.

corrected for body surface area were  $23 \pm 19$  ml/min/m<sup>2</sup> in the normal vessels and  $19 \pm 16$  ml/min/m<sup>2</sup> in the diseased vessels. In the patient with an occluded LAD and collaterals, the volume flow in the GCV was 7 ml/min/m<sup>2</sup>. MR is a unique tool for noninvasive simultaneous measurement of the flow pattern and volume flow in the GCV and the LAD, showing a clear distinction between arterial and venous flow.

**Key Words:** Coronary vessels; Flow dynamics; Magnetic resonance imaging; Velocity quantification

## INTRODUCTION

Quantification of absolute coronary artery and collateral flow to myocardial regions supplied by severely diseased or totally occluded coronary arteries remains difficult to assess in humans. Quantitative measurement of myocardial perfusion is accomplished with positron emission tomography, but this method is not yet widely available. The feasibility has been demonstrated to quantify absolute phasic and mean flow in the coronary arteries (1–3) and veins (4,5) noninvasively using magnetic resonance (MR) phase-contrast velocity measurements. In animals, this method has been validated in comparison with ultrasound transit time measurements (2,6,7) and in humans in comparison with Doppler guidewire measurements (8–10). An excellent correlation was reported between MR flow measurements in the coronary sinus and assessment of left ventricular myocardial perfusion using positron emission tomography (11). Application of these techniques in the coronary sinus may serve as an indicator of global myocardial perfusion of the left ventricle in healthy subjects (4) and in patients with diffusely abnormal left ventricular function, for example hypertrophic cardiomyopathy (12). When regional differences in coronary flow and metabolism occur, coronary sinus sampling is likely to be inadequate.

The left anterior descending coronary artery (LAD) and its diagonal and septal branches predominantly perfuse the anteroseptal and anterolateral left ventricular wall and drain through the great cardiac vein (GCV). Direct determination of volume flow in the LAD by MR estimates the anterior left ventricular regional flow. GCV flow can be used as an indirect index of anterior left ventricular regional flow (13), the difference between coronary sinus and GCV flow providing an estimate of inferior left ventricular regional flow. The vessels run closely parallel to each other in the interventricular sulcus; usually the GCV is located lateral of the LAD. An early intersection of the GCV and the LAD can make the distinction difficult.

The aim of this study was to show the feasibility to distinguish both structures by the flow pattern and quantify the volume flow in the LAD and GCV simultaneously using a single noninvasive technique to obtain an index of regional anterior myocardial perfusion.

## MATERIALS AND METHODS

MR imaging was performed in 19 individuals; the study group characteristics are listed in Table 1. Eleven individuals, 5 men and 6 women with a mean age of 42 years, had a presumably normal LAD and 8 patients, 7 men and 1 woman with a mean age of 61 years, had a diseased LAD. The mean body surface area was 1.9 m<sup>2</sup> (range, 1.5–2.2). With exception of the healthy volunteers, all subjects underwent coronary angiography within 2 weeks of the MR scan. In patients with a diseased LAD, three suffered from angina and four sustained an anterior myocardial infarction treated with reperfusion therapy. In one patient (patient 15, Table 1) with sustained anterior infarction and not treated with reperfusion therapy, the LAD was occluded and angiographically significant collaterals were present from the right coronary artery to the LAD perfusion territory. Patients were ineligible for enrollment if they had a contraindication for MR imaging (pacemaker, intracranial metal, unstable medical condition, or claustrophobia) or cardiac arrhythmias interfering with adequate image acquisition. All subjects underwent phase-contrast velocity measurements in the LAD and GCV.

Imaging was performed on a 1.5-T whole body MR system (Vision, Siemens, Erlangen, Germany) using a phased array body coil and prospective electrocardiographic gating. First, MR angiography of the proximal coronary arteries was performed with a two-dimensional technique (14) (Fig. 1). Transverse slices were acquired with a breathhold technique during inspiration to visualize the coronary vessels. Differentiation between LAD and GCV was made by tracking connectivity of the LAD



**Table 1**  
*Clinical Characteristics of the Study Group*

Subjects	Age, Sex	Clinical Status	Coronary Angiogram
1	30, M	Healthy volunteer	Not performed
2	28, F	Healthy volunteer	Not performed
3	27, F	Healthy volunteer	Not performed
4	27, F	Healthy volunteer	Not performed
5	29, M	Ventricular tachycardia	LAD normal
6	60, M	Unstable angina pectoris	LAD 90%
7	50, M	Anterior infarction, thrombolysis	LAD 80%
8	60, M	Anterior infarction, primary PTCA	LAD < 50%
9	60, M	Unstable angina pectoris	LAD normal
10	60, M	Unstable angina pectoris	LAD 99%
11	60, M	Unstable angina pectoris	LAD 70%
12	53, F	Unstable angina pectoris	LAD normal
13	68, M	Unstable angina pectoris	LAD normal
14	68, M	Unstable angina pectoris	LAD normal
15	61, F	Anterior septal infarction, no treatment	LAD 100%
16	58, M	Old inferior, recent anterior septal infarction, thrombolysis	LAD 90%
17	48, M	Anterior septal infarction, primary PTCA	LAD < 50%
18	49, F	Unstable angina pectoris	LAD normal
19	28, F	Healthy volunteer	Not performed

M, male; F, female; PTCA, percutaneous transluminal coronary angioplasty.

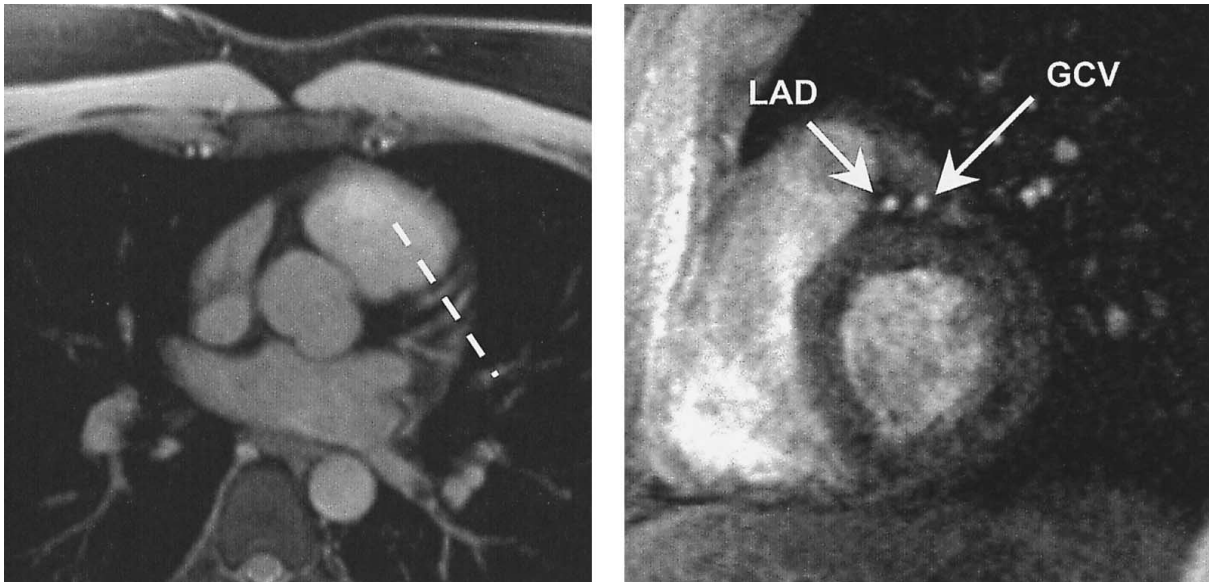


**Figure 1.** A two-dimensional MR angiogram (left panel) showing the LAD and GCV in a transverse plane. The dashed line indicates the acquisition plane of the MR flow velocity measurement. The right panel shows cross-sections of the LAD and GCV in the interventricular sulcus.

Copyright © Marcel Dekker, Inc. All rights reserved.

to the aortic root on series of consecutive MR angiographic images. Because both vessels run closely parallel to each other in the interventricular sulcus, MR phase-contrast velocity measurements can be performed in a single plane perpendicular to both structures within one breathhold (spatial resolution,  $0.9 \times 1.5 \times 6 \text{ mm}^3$ ) (2,5). Thus, a cross-sectional view of both coronary vessels is obtained perpendicular to the direction of flow, minimizing in-plane motion and partial volume effects. Figure 2 illustrates these cross-sections at two different phases of the cardiac cycle; the end-systolic and the mid-diastolic

phase. In both phases the magnitude and the phase velocity encoded images are shown. A segmented k-space technique (15,16) was used to obtain five phase-encoding steps for each frame within the cardiac cycle, resulting in an acquisition window of 105 msec. Other imaging parameters included a temporal resolution of 125 msec (five to nine phases), a flip angle of 30 degrees, a field of view of  $200 \times 200 \text{ mm}^2$ , an echo time of 5 msec, and a scan duration of 27 heart beats. Because of prospective electrocardiographic gating, no data were acquired from the last 50–150 msec of the cardiac cycle. Before every

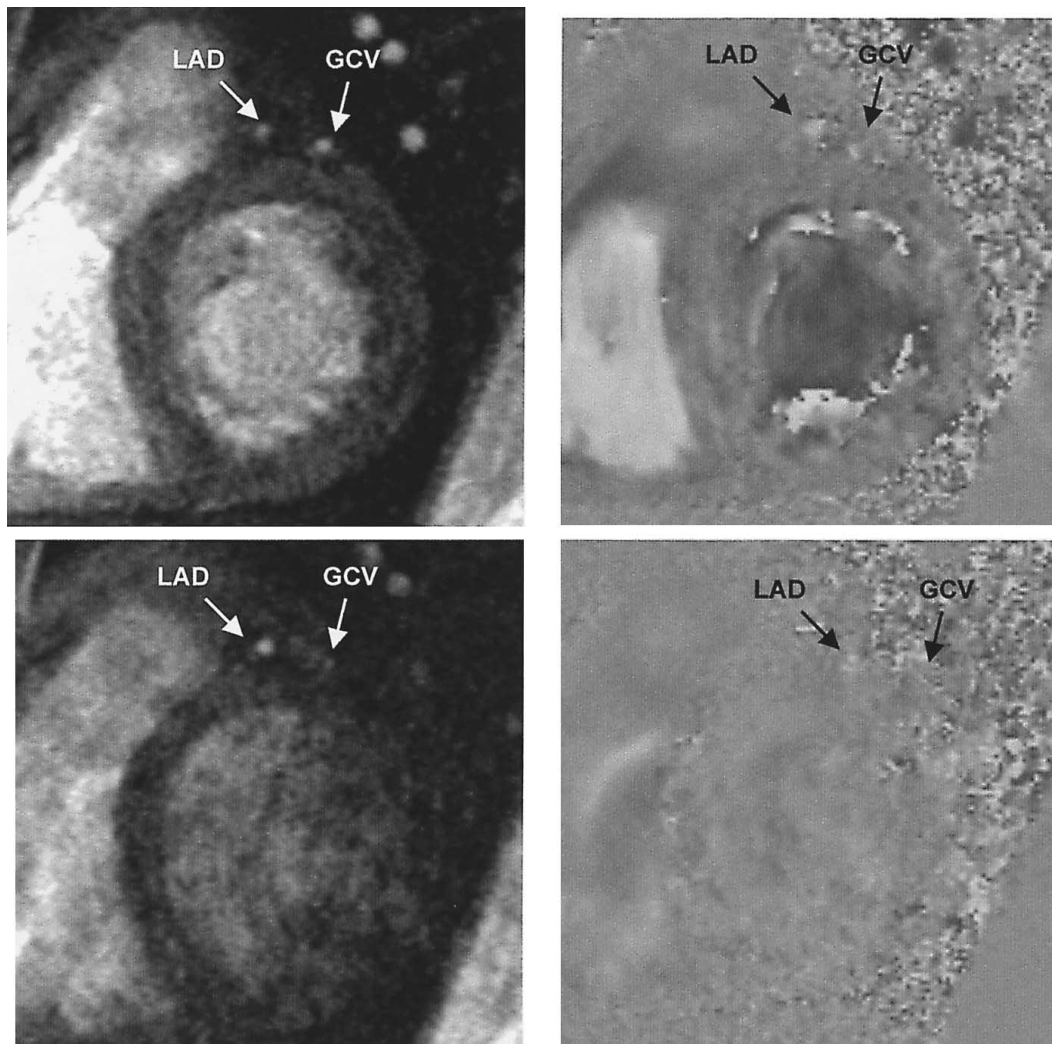


**Figure 2.** Images obtained perpendicular to the GCV and LAD, similar to Fig. 1. Magnitude images are on the left, and phase velocity encoded images are on the right. The upper images were obtained at end-systole, when both the LAD and GCV are clearly visible. The lower images were obtained in mid-diastole, predominantly depicting the LAD.

frame a fat saturation prepulse was applied. The encoding velocity was set to 75 cm/sec, resulting in a velocity window of  $-75$  to  $75$  cm/sec. Heart rate and systemic arterial pressure were monitored and recorded during the imaging procedure. Flow mapping in both structures took approximately 10 min per patient.

Flow analysis was performed with the FLOW<sup>®</sup> software package (Department of Radiology, Leiden University Medical Center, The Netherlands). The contour of the cross-sectioned LAD was visually determined on a magnitude image at mid-diastole, the phase of the cardiac cycle in which the highest image quality was obtained. The contour of the GCV was more evident in the end-systolic phase (Fig. 2). The area of the region of interest

was kept constant over the cardiac cycle and repositioned at each time frame on the magnitude image. A 400% magnification was used during image analysis. The averaged velocity was measured within each contour on the corresponding phase-contrast image. The velocity of the myocardial motion was obtained by drawing a contour in the myocardial tissue close to the vessel of interest. To correct for cardiac motion, the velocity within this contour was subtracted from the flow velocity within the vessel, resulting in a net forward velocity. The product of area and velocity yields instantaneous volumetric blood flow. Plots were made of phasic volume of blood flow versus time in the cardiac cycle. Because a prospectively triggered electrocardiographic gating technique

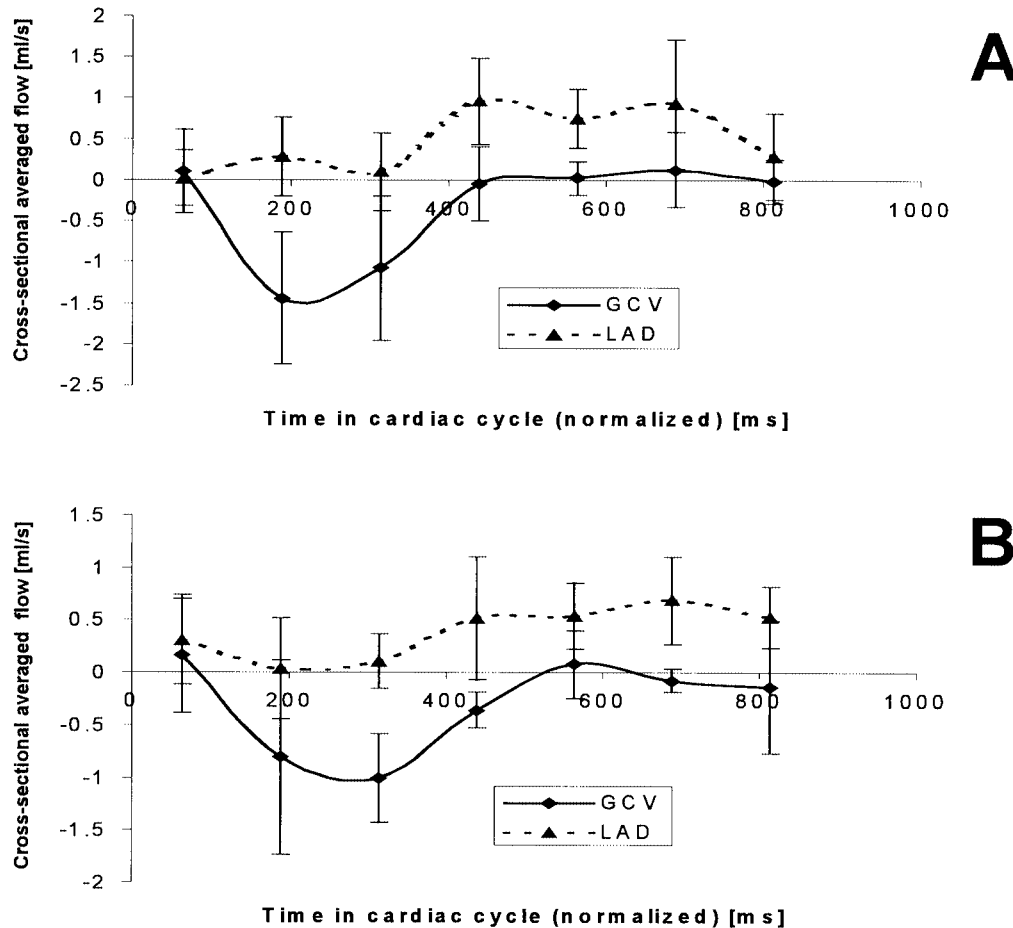


**Figure 3.** The cross-sectional averaged volume flow in the LAD versus the GCV in 11 subjects with a normal LAD (A) and in 7 patients with coronary artery disease (B). Mean values with SDs are shown. All measurements are normalized to heart rates of 60 beats/min, corrected for the duration of systole and diastole (16). Subsequently, data points within time intervals were averaged, resulting in a variable number of subjects per data point shown (A:  $9 \pm 2$ ; B:  $6.1 \pm 1.2$ ).

was used, no measurements could be obtained during the final 50 msec of the cardiac cycle. To calculate the intra- and interobserver variability, flow analysis was performed by a second observer and repeated by the first observer. Both were blinded for the achieved results.

All results are presented as means  $\pm$  SD. Statistical significance of difference in volume flow was determined with an unpaired Student's *t*-test, and  $p < 0.05$  was considered significant. For the intra- and interobserver variability, Bland Altman analysis was used. To compare LAD to GCV, flow linear regression was performed. The correlation coefficient was tested for significant difference from zero using the Student's *t*-test.

### RESULTS

MR imaging studies were well tolerated by all subjects. During the studies the heart rate was on average  $62 \pm 12$  beats/min (range, 44–86). The systolic blood pressure was  $122 \pm 16$  mm Hg in the diseased LAD group and  $130 \pm 28$  mm Hg in the normal LAD group. The diastolic blood pressure was  $73 \pm 8$  mm Hg in the diseased LAD group and  $71 \pm 15$  mm Hg in the normal LAD group.

The cross-sectional area of the LAD was  $19 \pm 4$  mm<sup>2</sup> (range, 9–33) and of the GCV  $17 \pm 5$  mm<sup>2</sup> (range, 11–27). Flow measurements allowed differentiating the LAD and GCV by two characteristics. First, the arterial flow pattern was mainly diastolic in contrast to the venous flow pattern, which was mainly systolic (Fig. 3). Second, the time-averaged volume flow in the LAD was in opposite direction of flow in the GCV. These criteria appear to be valid in all individual subjects. Figure 3A represents the volume flow of the group of patients with a nondiseased LAD. The flow is mainly diastolic in the LAD and systolic in the GCV. Figure 3B represents the volume flow of the group of patients with a diseased LAD, demonstrating a similar flow pattern in the LAD and the GCV. To compare the flow patterns in the LAD and the

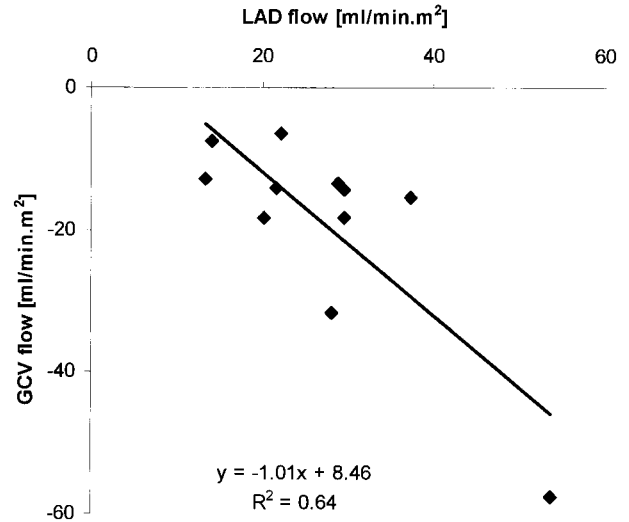


**Figure 4.** Scatter plot showing the relationship between the flow volume per minute corrected for body surface area in the LAD and GCV in 11 subjects with a presumably normal LAD. Collateral supply is not expected in this subgroup.

GCV, the heart rates of the subjects were normalized to 60 beats/min.

The volume flow measurement in the LAD corrected for body surface area in the normal LAD group ( $n = 11$ ) was  $31 \pm 15$  ml/min/m<sup>2</sup> and in the diseased nonoccluded LAD group ( $n = 7$ ) was  $21 \pm 10$  ml/min/m<sup>2</sup> (difference not significant). The volume flow measurement in the GCV corrected for body surface area in the normal LAD group was  $23 \pm 19$  ml/min/m<sup>2</sup> and in the diseased LAD group was  $19 \pm 16$  ml/min/m<sup>2</sup> (difference not significant). The intraobserver variability for the volume flow determination was  $0.1 \pm 0.2$  ml/sec; the interobserver variability was  $0.1 \pm 0.3$  ml/sec. In the patient with an occluded LAD and collateral supply, the volume flow in the GCV was 7 ml/min/m<sup>2</sup> (Table 2). Figure 4 shows the relation between the GCV flow and the LAD flow. Only the subjects with a presumably normal LAD are included;

**Table 2**

*Absolute Average Volume Flow in the LAD and GCV Plus SD Corrected for Body Surface Area*

	LAD (ml/min/m <sup>2</sup> )	GCV (ml/min/m <sup>2</sup> )
Normal ( $n = 11$ )	$31 \pm 15^*$	$23 \pm 19^\dagger$
Diseased ( $n = 7$ )	$21 \pm 10$	$19 \pm 16$
LAD occlusion + collateral supply		7

\**p* normal vs. diseased (= 0.19), †*p* normal vs. diseased (= 0.67).

in this subgroup without collateral supply a relation between the LAD and GCV flow is to be expected. A significant correlation of -0.80 was found ( $p = 0.003$ ). The slope and intercept were not different from 1 and 0, respectively.

## DISCUSSION

We demonstrated the feasibility to distinguish the flow in the LAD and GCV and quantify the volume flow in both vessels using cine MR velocity mapping. The method may serve to estimate the volume flow that perfuses and drains the anterior myocardial region. Differentiation between the GCV and the LAD cannot only be derived from connectivity to the aortic root but also by the direction and phase of the flow pattern. In this study we observed a systolic flow pattern in the GCV, which was also present in individuals with a highly stenotic LAD. This characteristic flow pattern in the GCV, consisting of a predominant systolic wave and small waves resulting from the atrial and isovolumetric contraction, has previously been described in animal studies (17,18). The systolic flow pattern in the GCV and its reverse relationship to the adjacent LAD has been noted in a human by Keegan et al. (5), albeit without correction for through-plane velocity of the vessels themselves.

The advantage of MR imaging in contrast to other imaging techniques is the potential to noninvasively measure volume flow in addition to flow velocity. The volume flow data from both vessels in this study are acquired simultaneously. Thus, the comparison between the measured flow rates is not influenced by variability of heart rate and blood pressure. Simultaneous data acquisition of the volume flow in the GCV measured with the thermodilution technique and LAD peak flow velocity measured with a Doppler guidewire was described in a previous study (19). Because of the difference in acquired parameters, conclusions about quantification and comparison of flow could not be made.

The feasibility and validation to quantify absolute phasic and mean flow in the coronary arteries and veins noninvasively with MR was demonstrated in several studies (1–5). Although the method has been validated in animals and in humans, MR flow measurements are technically restricted because of the small size, tortuosity and motion of the coronary artery, and acceleration and non-uniformity of high flow in stenosed arteries. The long imaging time requires patients to be cooperative and skillful in repetitive breathholding to avoid blurring of the images.

The single breathhold phase velocity mapping technique used in this study has some limitations. First, it requires long breathholding (20–35 sec), which may be difficult to obtain in every patient. Thereby the position of breathholding can vary, which results in a different image position than planned. An improvement could be monitoring of breathhold position to check for breathhold consistency. Second, the technique has a somewhat larger acquisition window than was suggested by Hofman et al. (20), which can be the explanation of the overestimation of vessel diameter. A shorter acquisition window will result in a higher accuracy, but this could not be obtained on the system used within a breathhold period. The motion-induced blurring results in an overestimation of the vessel cross-section. In the volume flow determination, this is partly compensated by the decreased averaged velocity. Third, the current in-plane spatial resolution is limited for measuring the arterial lumen cross-sectional area; a higher spatial resolution would be preferable to limit partial volume effects (21). The slice thickness (6 mm) does not influence the measurement of through-plane velocity strongly, because the imaged plane was positioned perpendicular to a relative straight segment of the proximal LAD and GCV. Furthermore, the flow data are subject to intra- and interobserver variability, because of the manual tracing of the vessel cross-section. Although the observer variability found in this study and in a previously reported study (10) was reasonable, an objective method for flow quantification should be further explored (7). Finally, the signal-to-noise ratio in the velocity maps was not such a limitation. The Gaussian noise in the images resulted into a volume flow error of about 0.1 ml/sec at an individual cardiac phase (22).

In our opinion a comparison of absolute magnitude volume flow measurements between the patients and the presumably normal subjects should not be performed. First, the hemodynamic conditions such as blood pressure and heart rate vary between subjects. A relative parameter such as coronary flow reserve or the ratio of GCV flow to LAD flow may circumvent this. Second, the range of the volume flow measurements in the LAD and GCV was relatively large, which is probably due to the small numbers of subjects and a nonuniform medical therapy and medical history. This may also explain the large SD in this group. As expected, a significant correlation was found between volume flow in the GCV to volume flow in the LAD (Fig. 4). This relationship was suggested in several studies (13,19) in which coronary venous flow was used as an index of regional anterior myocardial flow. Contrarily, Cohen et al. (23) did not find a reliable interdependence of coronary arteries and veins in dogs.



This contradictory finding might be explained by the difference of the collateral network, which is much more developed in the dog than in humans.

A clinical application of measuring GCV flow might be the assessment of collateral supply in case of occlusion of the LAD. This has been previously described with an invasive thermodilution method (24). In our study, the single patient with an occluded LAD and collateral supply demonstrated persisting GCV flow of approximately one third of normal values. This is more than would be expected on the basis of Thebesian venous drainage and may well reflect additional drainage of the collateral supply. Only volume flow at rest was measured. However, the potential of MR to obtain peak volume flow during pharmacologic stress may be used to determine coronary or venous flow reserve noninvasively (1,10). Also, GCV flow may provide more insights in the prognosis of patients with an acute myocardial infarction and early reperfusion and possibly serve as an index of the no-reflow phenomenon (25,26). Progressive decrease in GCV flow has been reported to be related to a decrease in left ventricular ejection fraction at follow-up (25,26).

In conclusion, the flow in the GCV is mainly systolic and points in the inverse direction of flow in the LAD. Although the patient group was small and suffered from variable ischemic events, the described flow pattern in the vessels appears to be consistent. MR is a unique tool for noninvasive simultaneous measurement of the flow pattern and volume flow in the GCV and the LAD.

#### ACKNOWLEDGMENT

Supported by a grant from the Netherlands Heart Foundation.

#### REFERENCES

1. Hundley, W.G.; Lange, R.A.; Clarke, G.D.; Meshack, B.M.; Payne, J.; Landau, C.; McColl, R.; Sayard, D.E.; Willett, D.L.; Willard, J.E.; Hillis, L.D.; Peshock, R.M. Assessment of Coronary Arterial Flow and Flow Reserve With Magnetic Resonance Imaging. *Circulation* **1996**, *93*, 1502–1508.
2. Clarke, G.D.; Eckels, R.; Chaney, C.; Smith, D.; Dittrich, J.; Hundley, W.G.; NessAiver, M.; Li, H.F.; Parkey, R.W.; Peshock, R.M. Measurement of Absolute Epicardial Coronary Artery Flow and Flow Reserve Using Breathhold Cine Phase-Contrast Magnetic Resonance Imaging. *Circulation* **1995**, *91*, 2627–2634.
3. Clarke, G.D.; Hundley, W.G.; McColl, R.W.; Eckels, R.; Smith, D.; Chaney, C.; Li, H.F.; Peshock, R.M.

Velocity-Encoded, Phase-Difference Cine MRI Measurements of Coronary Artery Flow: Dependence of Flow Accuracy on the Number of Cine Frames. *J. Magn. Reson. Imaging* **1996**, *6*, 733–742.

4. van Rossum, A.C.; Visser, F.C.; Hofman, M.B.M.; Galjee, M.A.; Westerhof, N.; Valk, J. Global Left Ventricular Perfusion: Noninvasive Measurement with Cine MR Imaging and Phase Velocity Mapping of Coronary Venous Outflow. *Radiology* **1992**, *182*, 685–691.
5. Keegan, J.; Firmin, D.; Gatehouse, P.; Longmore, D. The Application of Breathhold Phase Velocity Mapping Techniques to the Measurement of Coronary Artery Blood Flow Velocity: Phantom Data and Initial In Vivo Results. *Magn. Reson. Med.* **1994**, *31*, 526–536.
6. Hofman, M.B.M.; Visser, F.C.; van Rossum, A.C.; Vink, G.Q.M.; Sprenger, M.; Westerhof, N. In Vivo Validation of Magnetic Resonance Volume Flow Measurements With Limited Spatial Resolution in Small Vessels. *Magn. Reson. Med.* **1995**, *33*, 778–784.
7. Wedding, K.L.; Grist, T.M.; Folts, J.D.; Maalej, N.; Vigen, K.K.; Peters, D.C.; Osman, H.; Mistretta, C.A. Coronary Flow and Flow Reserve in Canines Using MR Phase Difference and Complex Difference Processing. *Magn. Reson. Med.* **1998**, *40*, 656–665.
8. Sakuma, H.; Blake, L.M.; Amidon, T.M.; O'Sullivan, M.; Szolar, D.H.; Furber, A.P.; Bernstein, M.A.; Foo, T.K.; Higgins, C.B. Coronary Flow Reserve: Noninvasive Measurement in Humans With Breathhold Velocity-Encoded Cine MR Imaging. *Radiology* **1996**, *98*, 745–750.
9. Nagel, E.; Bornstedt, A.; Hug, J.; Schnackenburg, B.; Wellnhofer, E.; Fleck, E. Noninvasive Determination of Coronary Blood Flow Velocity With Magnetic Resonance Imaging: Comparison of Breathhold and Navigator Techniques With Intravascular Ultrasound. *Magn. Reson. Med.* **1999**, *41*, 544–549.
10. Hundley, W.G.; Hamilton, C.A.; Clarke, G.D.; Hillis, L.D.; Herrington, D.M.; Lange, R.A.; Applegate, R.J.; Thomas, M.S.; Payne, J.; Link, K.M.; Peshock, R.M. Visualization and Functional Assessment of Proximal and Middle Left Anterior Descending Coronary Stenoses in Humans With Magnetic Resonance Imaging. *Circulation* **1999**, *99*, 3248–3254.
11. Schwitter, J.; DeMarco, T.; Kneifel, S.; von Schulthess, G.K.; Jorg, M.C.; Arheden, H.; Ruhm, S.; Stumpe, K.; Buck, A.; Parmley, W.W.; Luscher, T.F.; Higgins, C.B. Magnetic Resonance-Based Assessment of Global Coronary Flow and Flow Reserve and Its Relation to Left Ventricular Functional Parameters: A Comparison With Positron Emission Tomography. *Circulation* **2000**, *101*, 2696–2702.
12. Kawada, N.; Sakuma, H.; Yamakado, T.; Takeda, K.; Isaka, N.; Nakano, T.; Higgins, C.B. Hypertrophic Cardiomyopathy: MR Measurement of Coronary Blood Flow and Vasodilator Flow Reserve in Patients and Healthy Subjects. *Radiology* **1999**, *211*, 129–135.

13. Feldman, R.L.; Conti, C.R.; Pepine, C.J. Regional Venous Flow Responses to Transient Coronary Artery Occlusion in Human Beings. *J. Am. Coll. Cardiol.* **1983**, *2*, 1–10.
14. Edelman, R.R.; Manning, W.J.; Burstein, D.; Paulin, S. Coronary Arteries Breathhold MR Angiography. *Radiology* **1991**, *181*, 641–643.
15. Atkinson, D.J.; Edelman, R.R. Cineangiography in the Heart Is a Single Breathhold Technique With a Segmented turboFLASH Sequence. *Radiology* **1991**, *178*, 357–360.
16. Hofman, M.B.M.; van Rossum, A.C.; Sprenger, M.; Westerhof, N. Assessment of Flow in the Right Human Coronary Artery by Magnetic Resonance Phase Contrast Velocity Measurement: Effects of Cardiac and Respiratory Motion. *Magn. Reson. Med.* **1996**, *35*, 521–523.
17. Canty, J.M.J.; Brooks, A. Phasic Volumetric Coronary Venous Outflow Patterns in Conscious Dogs. *Am. J. Phys.* **1990**, *258*, H1457–H1463.
18. Mito, K.; Ogasawara, Y.; Hiramitsu, O.; Tsujioka, K.; Kajiyama, F. A Laser Doppler Catheter for Monitoring Both Phasic and Mean Coronary Vein Flow. *Heart Vessels* **1990**, *6*, 1–8.
19. Rossen, J.D.; Oskarsson, H.; Stenberg, R.G.; Braun, P.; Talman, C.L.; Winniford, M.D. Simultaneous Measurement of Coronary Flow Reserve by Left Anterior Descending Coronary Artery Doppler and Great Cardiac Vein Thermodilution Methods. *J. Am. Coll. Cardiol.* **1992**, *20*, 402–407.
20. Hofman, M.B.; Wickline, S.A.; Lorenz, C.H. Quantification of In-Plane Motion of the Coronary Arteries During the Cardiac Cycle: Implications for Acquisition Window Duration for MR Flow Quantification. *J. Magn. Reson. Imaging* **1998**, *8*, 568–576.
21. Tang, C.; Blatter, D.D.; Parker, D.L. Accuracy of Phase-Contrast Flow Measurements in the Presence of Partial-Volume Effects. *J. Magn. Reson. Imaging* **1993**, *3*, 377–385.
22. Conturo, T.E.; Smith, G.D. Signal-To-Noise in Phase Angle Reconstruction: Dynamic Range Extension Using Phase Reference Offsets. *Magn. Reson. Med.* **1990**, *15*, 420–437.
23. Cohen, M.V.; Matsuki, T.; Downey, J.M. Pressure-Flow Characteristics and Nutritional Capacity of Coronary Veins in Dogs. *Am. J. Phys.* **1988**, *255*, H834–H846.
24. Feldman, R.L.; Pepine, C.J. Evaluation of Coronary Collateral Circulation in Conscious Humans. *Am. J. Cardiol.* **1984**, *53*, 1233–1238.
25. Nicklas, J.M.; Diltz, E.A.; O'Neill, W.W.; Bourdillon, P.D.; Walton, J.A.J.; Pitt, B. Quantitative Measurement of Coronary Flow During Medical Revascularization (Thrombolysis or Angioplasty) in Patients With Acute Infarction. *J. Am. Coll. Cardiol.* **1987**, *10*, 284–289.
26. Komamura, K.; Kitakaze, M.; Nishida, K., et al. Progressive Decreases in Coronary Vein Flow During Reperfusion in Acute Myocardial Infarction: Clinical Documentation of the No Reflow Phenomenon After Successful Thrombolysis. *J. Am. Coll. Cardiol.* **1994**, *24*, 370–377.

Received May 12, 2000

Accepted October 25, 2000



## **Request Permission or Order Reprints Instantly!**

Interested in copying and sharing this article? In most cases, U.S. Copyright Law requires that you get permission from the article's rightsholder before using copyrighted content.

All information and materials found in this article, including but not limited to text, trademarks, patents, logos, graphics and images (the "Materials"), are the copyrighted works and other forms of intellectual property of Marcel Dekker, Inc., or its licensors. All rights not expressly granted are reserved.

Get permission to lawfully reproduce and distribute the Materials or order reprints quickly and painlessly. Simply click on the "Request Permission/Reprints Here" link below and follow the instructions. Visit the [U.S. Copyright Office](#) for information on Fair Use limitations of U.S. copyright law. Please refer to The Association of American Publishers' (AAP) website for guidelines on [Fair Use in the Classroom](#).

The Materials are for your personal use only and cannot be reformatted, reposted, resold or distributed by electronic means or otherwise without permission from Marcel Dekker, Inc. Marcel Dekker, Inc. grants you the limited right to display the Materials only on your personal computer or personal wireless device, and to copy and download single copies of such Materials provided that any copyright, trademark or other notice appearing on such Materials is also retained by, displayed, copied or downloaded as part of the Materials and is not removed or obscured, and provided you do not edit, modify, alter or enhance the Materials. Please refer to our [Website User Agreement](#) for more details.

**[Order now!](#)**

Reprints of this article can also be ordered at

<http://www.dekker.com/servlet/product/DOI/101081JCMR100107471>